# Interactions of photons with matter and shape of spectra in X/γ-ray spectrometry

## 1. Interactions of photons with matter

Interactions are all processes that change the energy and/or the direction of the photon and will have direct influence on the shape of photon spectra. According to Bragg's law, the attenuation of a collimated photon beam arriving under normal incidence on a material of thickness x follows an exponential law (cf. Figure 13):

$$I = I_0 e^{-\mu x}$$

$I_0$ and $I$ represent respectively the incident and transmitted photon fluxes, $x$ is the material thickness (cm) and $\mu$ is the linear attenuation coefficient which reflects the interaction probability of one photon per unit length, expressed in $cm^{-1}$. This linear attenuation coefficient is related to the interaction cross-section (microscopic parameter) and depends on the material composition and the photon energy. Attenuation coefficients can be obtained from tables such as the NIST XCOM (M.J. Berger, 2010) for elements or mixtures with well-known composition. For mixtures of unknown composition or for the sake of accuracy, a dedicated facility has been set up at LNHB to directly measure the linear attenuation coefficient of a material (see § 5). The main processes of interaction of photons with matter are the following:

- Photoelectric absorption,
- Compton scattering,
- Pair production,
- Rayleigh scattering.

The Rayleigh scattering does not change the energy of the incident photons and consequently has no direct consequence on the detection. The occurrence of the other three types of interactions depends on the atomic number of the element and the energy of the incident photon (cf. Figure 1).

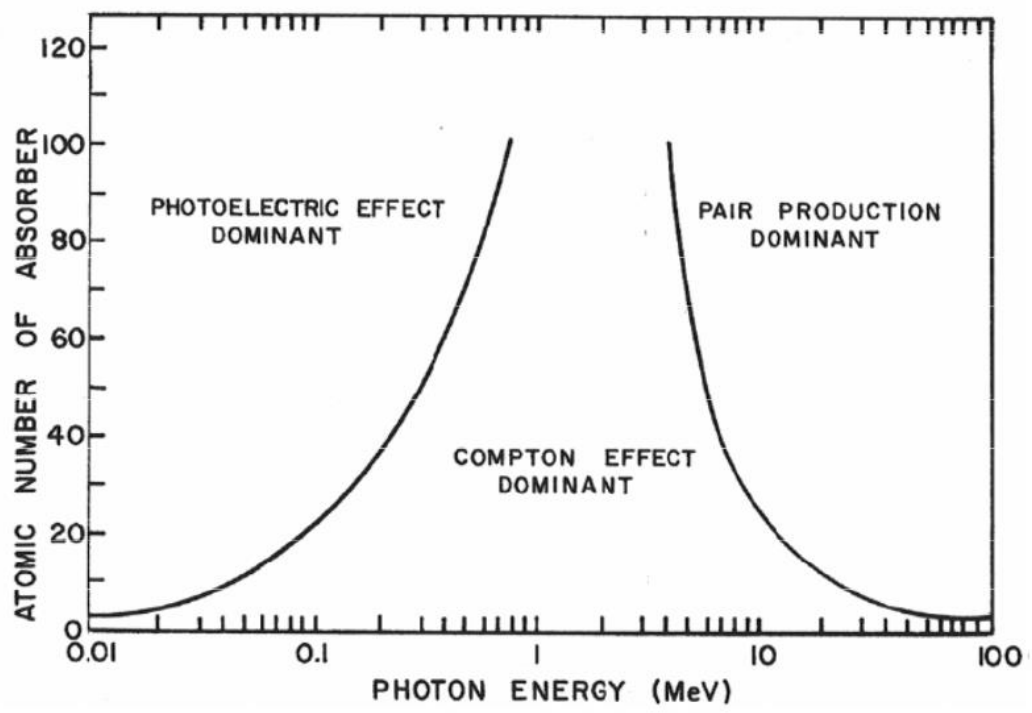


*Figure 1: Relative importance of the processes of interaction of photons with matter as a function of their energy and the medium composition (Evans, 1955).*

## 1.1. Photoelectric absorption

This process is the most interesting for gamma-ray spectrometry since the whole energy of the incident photon ($E = h\nu_0$) is transferred to an internal electron of an atom of the absorbing material (cf. Figure 2). The energy of the incident photon is totally absorbed by the electron which is then ejected (photoelectron) with a kinetic energy T depending on the energy of the incident photon and the binding energy of the corresponding electronic shell (or sub-shell).

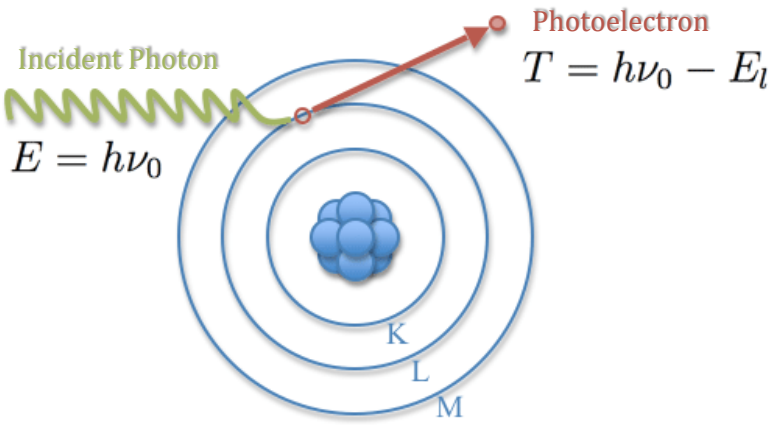


*Figure 2: Scheme of the photoelectric effect.*
*(Picture of Stan Nicol - web)*

*This phenomenon is dependent on the target atom and its cross-section has a strong dependence on the atomic number of the element, varying within $Z^5$. At low energy, the photoelectric cross-section shows discontinuities (cf.*

Figure 3) corresponding to the binding energies of the various electronic (sub-)shells.

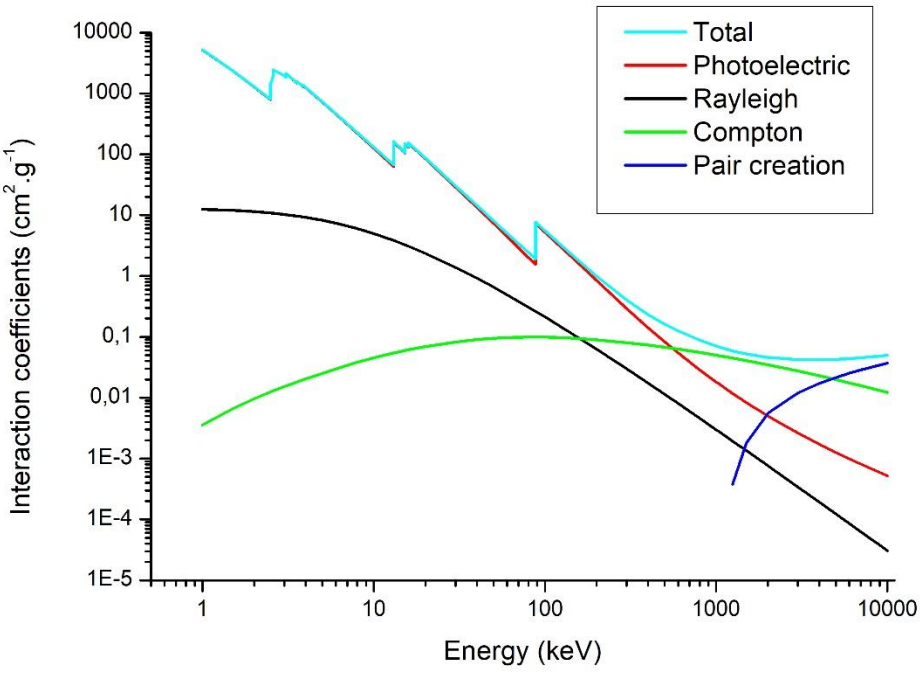


*Figure 3: Interaction coefficients as a function of energy for lead (XCOM).*

Any phenomenon extracting an electron shell is followed by the rearrangement of the electronic shells, filling the initial vacancy. There will either emission of fluorescent X-rays or Auger electrons whose energy is characteristic of the element.

## 1.2. Compton scattering

This process corresponds to the inelastic scattering of the incident photon onto an electron of an atom. It is one of the disturbing phenomena for photon spectrometry because it induces an important background in the spectrum. (cf. § 2). During this interaction, the incident photon is scattered at an angle θ with respect to its original direction and yields part of its energy to the electron. The latter is then ejected from the atom with kinetic energy *T*, at an angle *φ* with respect to the incident direction (cf. Figure 4). This type of interaction is little dependent on the environment, and evolves in *Z/A*.

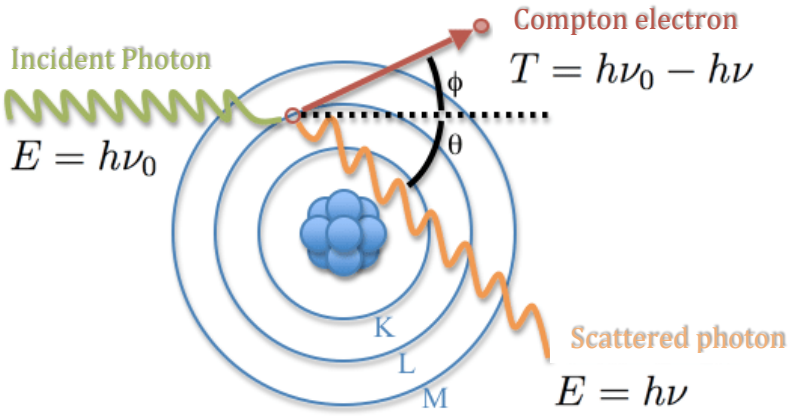


*Figure 4: Diagram of the Compton scattering.*
*(Picture of Stan Nicol - web)*

## 1.3. Pair production

In this process, the photon energy is converted into a positron-electron pair under the action of the intense Coulomb field around the atom nucleus (cf. Figure 5). This process is energetically possible only if the incident energy is greater than the sum of the masses of the electron and the positron, i.e. $E_{threshold} = 2m_ec^2 = 1.022\ MeV$.

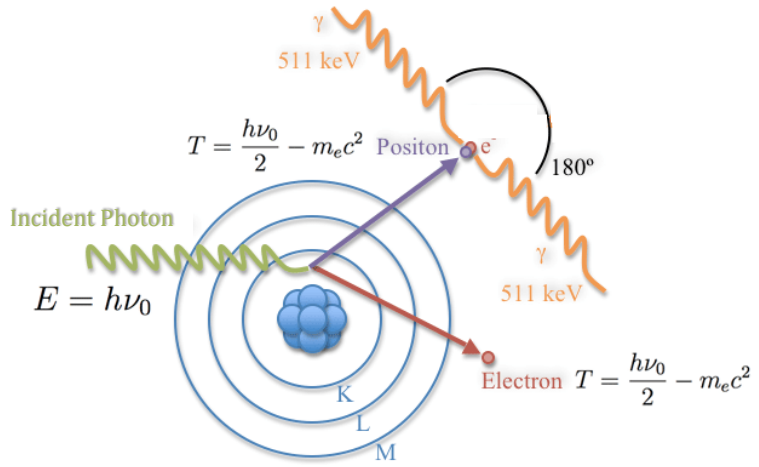


*Figure 5: Diagram of pair production followed by annihilation.*
*(Picture of Stan Nicol - web)*

The positron emitted during this process rapidly interacts with surrounding medium and annihilates with an electron, producing two 511-keV photons emitted at 180° from each other. The higher both the atomic number of the medium, proportional to $Z^2$, and the energy of the photons ($E > E_{threshold}$), the higher the probability of producing pairs. This phenomenon remains a problem for gamma-ray spectrometry, but it is useful in other specific fields (PET imaging).

### 1.4. Coherent scattering (Rayleigh or elastic scattering)

Coherent scattering transfers negligible energy to the atom, the photon is deviated from its initial trajectory without losing energy.

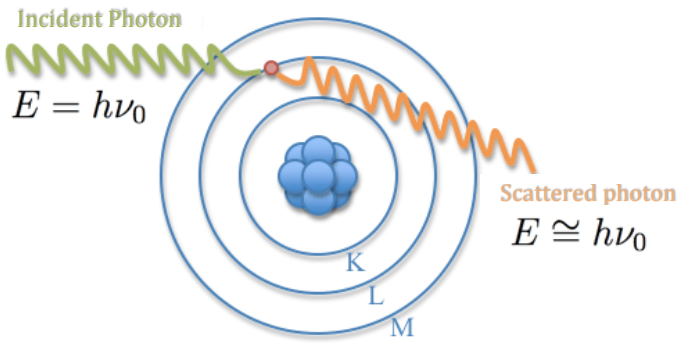


*Figure 6: Diagram of Rayleigh diffusion*
*(Picture of Stan Nicol - web)*

This type of interaction depends on the atomic number (function in $Z^2$); it has no impact on the spectra.

## 2. Measurement in gamma-ray spectrometry: shape of the spectra.

Regardless of the initial interaction process, the incident energy is fully or partially transmitted to an electron of the detector material. The successive interactions in the semiconductor material create a number of electron-hole pairs proportional to the energy initially transferred.

The collection of these secondary charges at the detector electrodes generates electrical pulses with an amplitude proportional to the energy of the primary electrons set in motion. All of this information constitutes the energy spectrum which is characterized in particular by full-energy peaks (position = energy, surface = activity) corresponding to the absorption of all the incident energy, by a single photoelectric

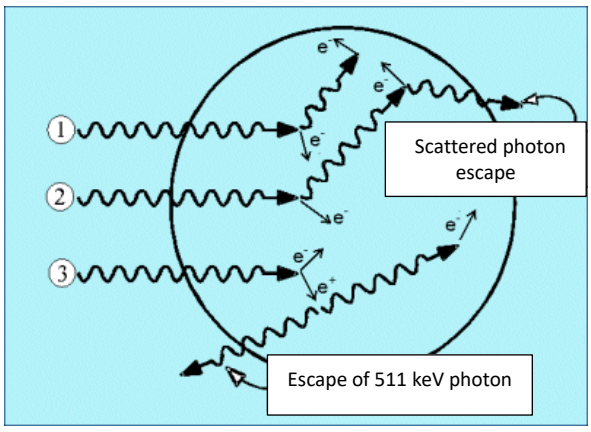


1. *Full absorption: contributes to full-energy peak,*
2. *Compton scattering and escape of scattered photons contribute to the continuous background*
3. *Pair production + escape of a 511 keV photon: contributes to the single escape peak*

*Figure 7: Examples of photon interactions in a detector.*

In addition to the full-energy peak, the spectra includes other peaks, which are identified and numbered in Figure 8 as follows:

- Peaks due to the escape of Ge K X-rays at *E*-9.9 keV **(1),**
- Peaks corresponding to the X-rays coming from the fluorescence of the materials surrounding the detector (most often the X-rays of lead **(2)**; here not very visible due to the X-rays of Bi-207),
- A continuous background corresponding to partial transfers of incident photon energy with the possibility of seeing the Compton edge **(4)** as well as the backscattered "peak"**(3)**,
- The annihilation peak (at 511 keV) **(5)** resulting from the detection of photons produced as a result of annihilation (following pair creation or beta-plus decay),
- Sum peaks depending on source activity and detection geometry (coincidence or pile-up) **(6)**,
- Possibly a continuous background related to the detection of high-energy electrons from the source **(7)** (possible if the detector window is thin),
- Peaks of single **(8)** and double **(9)** escape due to the pair production effect, if the initial energy is higher than 1022 keV.

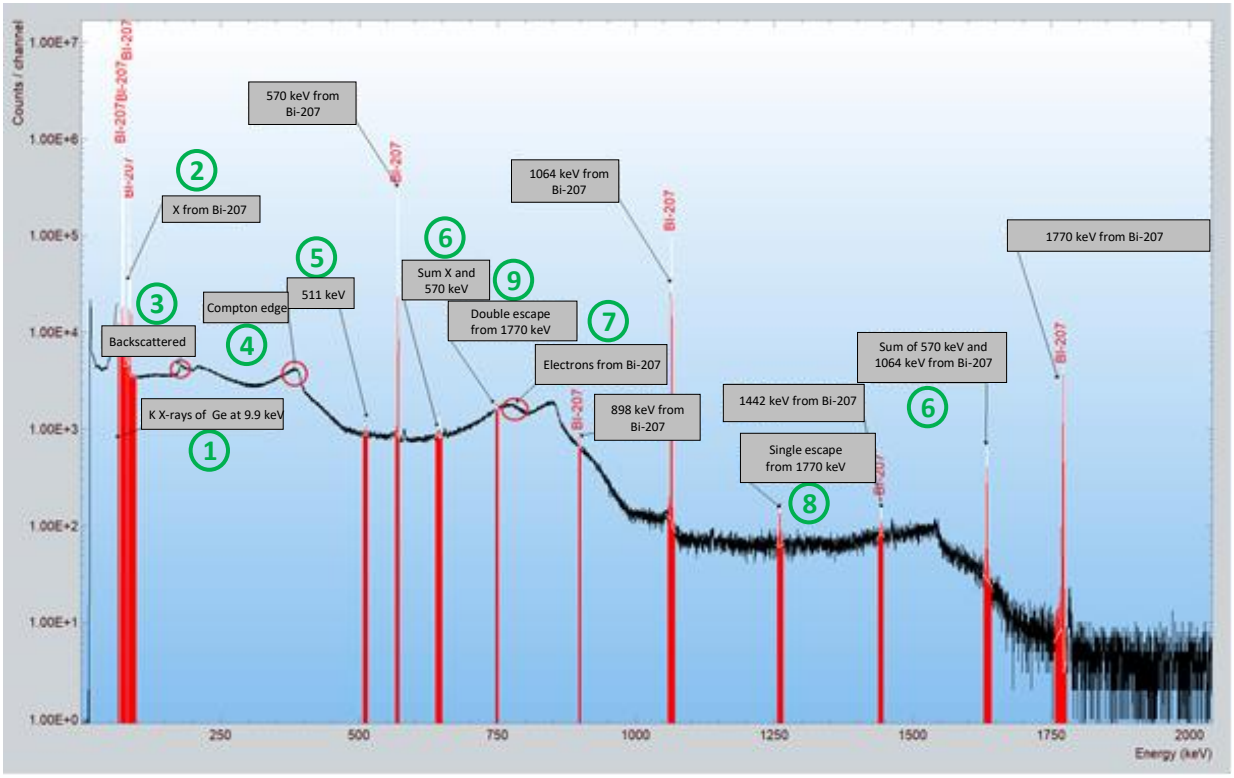


*Figure 8: Spectrum of a Bi-207 source where different possible interactions are shown.*

The relative intensity of the different components of the spectrum depends on the detection volume and surroundings of the detector.

## 3. Energy resolution of the spectra

The number of secondary electron-hole pairs (charge carriers obeys a statistical law that induces Gaussian widening of the peaks. In addition to this statistical component, effects due to electronics and charge collection defects lead to a variation in the amplitude of the recorded pulses and to a spreading of the peaks.

The performance of a detector is characterized in particular by its energy resolution, $\Delta E$, or the peak width at half maximum (FWHM = Full Width at Half Maximum), which influences the resolving power and the

detection limits. The resolution depends on the energy of the incident photons and the detector material. The resolving power of the detector is the ratio $\Delta E/E$ (%).

## 4. Detector calibration

The calibration of detectors is conventionally performed with radioactive sources of known activity. Detectors are energy calibrated using one or more sources whose radionuclides emit at known energies.

### 4.1. Full-energy peak efficiency

The full-energy peak efficiency, $\varepsilon(E)$, is the ratio of the number of events recorded in the full-energy peak to the number of photons emitted by the source (cf. Figure 9). $\varepsilon(E)$ depends on the detection geometry and the photon energy.

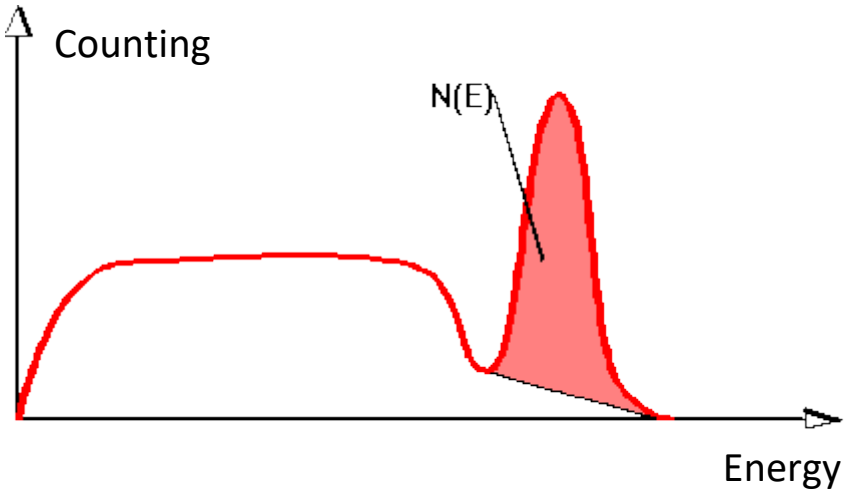


*Figure 9: Net peak area to determine the full-energy peak efficiency.*

$$\varepsilon(E) = \frac{N(E)}{F(E)}$$

*With* $F(E)$ the number of photons, with energy $E$,emitted by the source.

### 4.2. Total efficiency

The total efficiency, $\eta(E)$, is defined for a single gamma emitting radionuclide: it is the ratio of the number of events recorded in the whole spectrum (Figure 10) to the number of photons emitted by the source. The total efficiency depends on the detection **geometry** and the **energy** of the radiation. $\varepsilon(E)$ is used for quantitative analysis, $\eta(E)$ is necessary for the calculation of coincidence corrections.

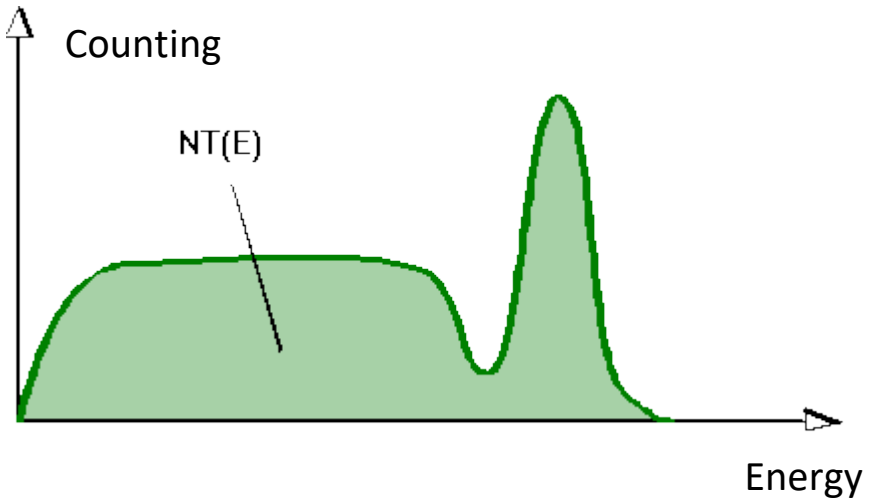


*Figure 10: Spectrum area to determine the total efficiency.*

$$\eta(E) = \frac{N_T(E)}{F(E)}$$

With $F(E)$ the number of photon with energy $E$ emitted by the source.

## 4.3. Geometrical and intrinsic efficiency

The full-energy peak efficiency is composed of a geometrical factor (source-detector geometry) and an intrinsic component depending on the energy of the incident radiation:

$$\varepsilon(E) = \varepsilon_G \times \varepsilon_I(E)$$

The geometrical efficiency, $\varepsilon_G$, independent of energy, is the ratio of the number of photons emitted in the direction of the detector, to the number of photons emitted in $4\pi$:

$$\varepsilon_G = \frac{\Omega}{4\pi}$$

$\Omega$ is the solid angle subtended by the source and the surface of the detector active volume; for a point source located at a distance *d* from the detector of radius $r$:

$$\Omega = 2\pi \left(1 - \frac{d}{\sqrt{d^2 + r^2}}\right)$$

The intrinsic efficiency $\varepsilon_I(E)$ depends on the energy: it is the ratio of the number of events detected under the full-energy peak *E*, to the number of photons reaching the detector surface.

## 4.4. Experimental determination of the detection efficiency

The experimental determination of the detection efficiency requires the use of a standard source(s), consisting of one or more radionuclides, placed at a distance *d* from the detection crystal (reference distance) (cf. Figure 11): a spectrum is recorded during the acquisition time *t*.

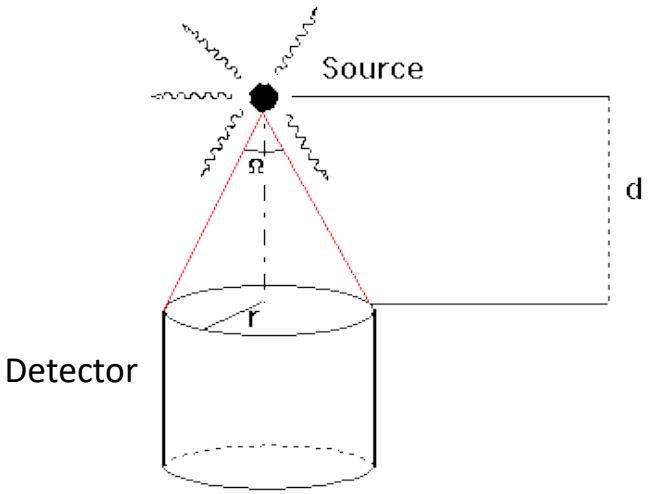


*Figure 11: Scheme of the solid angle.*

For each energy $E$ emitted by the source, there is a peak in the spectrum with an area $N(E)$ proportional to the number of photons emitted by the source and to the efficiency of the detector for the energy considered.

The full-energy peak efficiency, $\varepsilon(E)$ is determined according to:

$$\varepsilon(E) = \frac{N(E)}{A \times I(E) \times t}$$

- $N(E)$: number of moves recorded in the full-energy peak,
- $A$: activity of the source at the time of measurement (Bq),
- $I(E)$: emission intensity of the gamma-rays with energy *E*,
- $t$: acquisition time (live time),
- $\varepsilon(E)$: efficiency for energy E and source-detector in the calibration conditions (reference geometry)Depending on the experimental condition, the number of counts in the full-energy peak must be corrected by different factors:
- Decay during the acquisition time (short half-lives),
- Pile-up (high count rates),
- Coincidences (complex decay schemes)...

The efficiency must be determined with a calibration geometry similar to the measurement geometry. If no standards corresponding to the measurement geometry are available, an efficiency transfer factor must be computed and applied.

By using different radionuclides, experimental calibration data are obtained for a given geometry giving the full-energy peak efficiency as a function of the energy of each gamma (or X) emission considered (see Figure 12). A general curve is obtained by fitting a polynomial expression (for example) to the experimental values obtained using the standards.

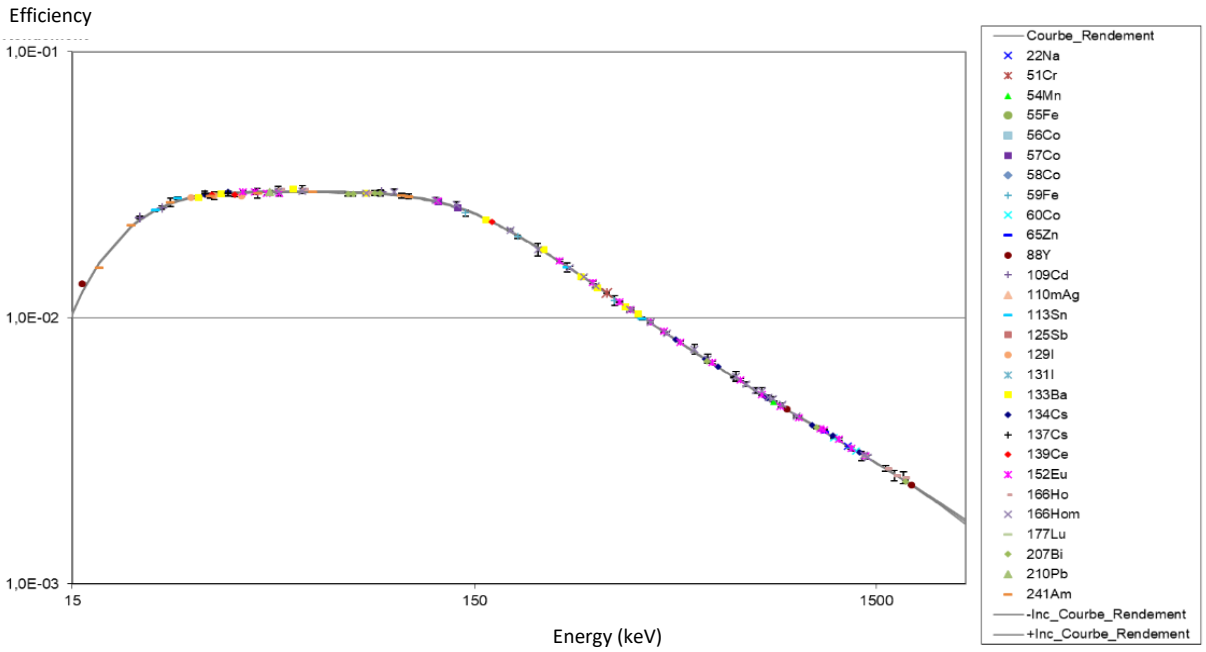


*Figure 12: Example of a full-energy efficiency curve for a N-type HPGe detector with a point source at 10 cm from the detector window.*

## 5. Measurement of attenuation coefficients

In the case of the measurements of volume samples, these may be in a different medium than the one used for the reference calibration. The self-attenuation of each material must therefore be taken into account, which is itself dependent on the attenuation coefficients. If the composition of the medium is well known, it is possible to use tables or software, such as XCOM software, to calculate the attenuation coefficients for a mixture of compounds.

However, this is not applicable for an environmental sample of unknown composition. Once the problem of homogeneity of the sample are removed, it is possible to directly measure the attenuation of this material by applying Beer-Lambert's law by considering a monochromatic photon beam (cf. Figure 13):

$$I(x) = I_0 \times e^{-\mu x} = I_0 \times e^{-\mu_\rho \rho x},$$

Where:

- $\mu$ ($cm^{-1}$) is the total linear attenuation coefficient of a material for an energy E,
- $x$ is the thickness of the material through which the beam passes,
- $\mu_\rho$ ($g^{-1}.cm^{-2}$) is the total mass attenuation coefficient of the material for an energy E,
- $\rho$ ($g.cm^{-3}$) is the density of the material.

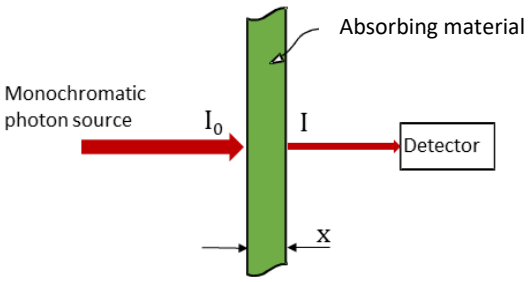


*Figure 13: Experimental conditions of the Beer-Lambert law.*

The attenuation coefficient of a material depends on the energy of the radiation and the atomic number (Z) of the medium. It is advisable to measure the attenuation of the material directly using a set-up as shown in Figure 14.

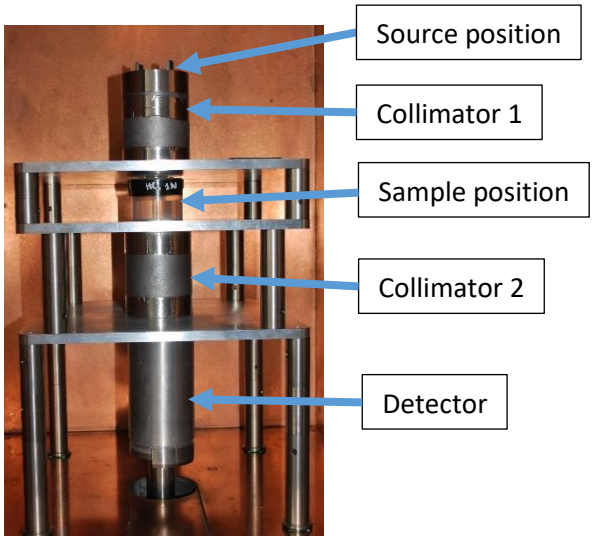


*Figure 14: Attenuation measurement of a material using a HPGe detector and collimated point sources.*

In this example, among the radiations emitted by a point source -consisting of $^{152}$Eu and $^{133}$Ba- a quasi-parallel beam is obtained by using a 15-cm thick lead collimator.

Two successive measurements must be carried out: one with an empty container, the other with the same container filled with a known thickness *x* of the material to be characterized.

$$\mu(E) = \frac{-\ln\left(\frac{N_{sample}}{N_{container}}\right)}{x},$$

with:

- $\mu(E)$ : linear attenuation coefficient of the material at energy E,
- $N_{sample}$ : count rate of the peak at energy E corrected for decay during the measurement and corrected to a chosen reference date when the container is filled with the sample material,
- $N_{container}$ : peak count rate at energy E corrected for decay during measurement and corrected to a chosen reference date when the empty container is placed,
- $x$ : thickness of sample.

Whenever possible, it is preferable to do this directly on the test sample to avoid problems with changing the density of the medium (filling problem in the container depending on the medium to be measured).

Figure 15 shows a result obtained with this installation for an epoxy resin sample manufactured at LNHB

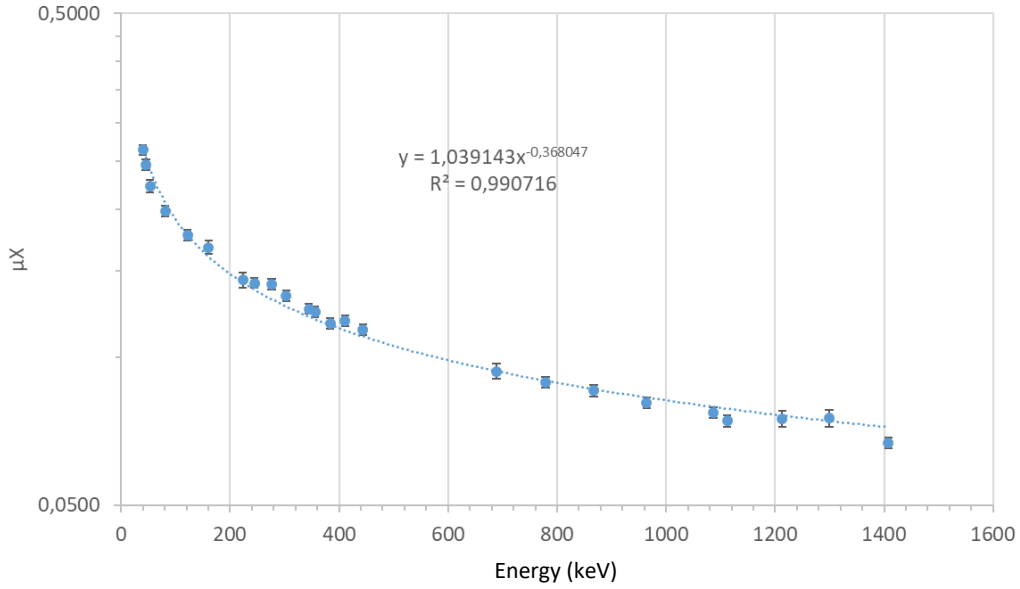


*Figure 15: Experimental attenuation coefficient of an epoxy resin.*

The drawback of this method is that it requires two successive acquisitions that are rather long (several days, even with sources with 1 MBq of activity, as in the present example). Another solution, for the lowest energies, is to use an X generator that allows to obtain different energy lines with a high photon flux.